Optik - International Journal for Light and Electron Optics 274 (2023) 170525

Contents lists available at ScienceDirect

Optik

journal homepage: www.elsevier.com/locate/ijleo

Conversion of a Gaussian-distributed circular beam to a flat-top-distributed square beam in laser shock processing based on a micro-lens array structure

Jinliang Han [a,b], Jun Zhang [a,*], Xiaonan Shan [a], Yawei Zhang [a], Hangyu Peng [a], Li Qin [a], Yannan Tan [c], Lijun Wang [a]

[a] Changchun Institute of Optics, Fine Mechanics and Physics, Chinese Academy of Sciences, Changchun 130033, China
[b] University of Chinese Academy of Sciences, Beijing 100049, China
[c] Dalian Institute of Chemical Physics, Chinese Academy of Sciences, Dalian, Liaoning 116023 China

ARTICLE INFO

Keywords:
Laser shock processing
High energy density
Flat-top-distributed laser beam
Beam homogenisation system
Micro-lens array

ABSTRACT

A novel beam homogenisation system based on a micro-lens array and beam expansion structure is proposed to convert a Gaussian-distributed circular beam to a flat-top-distributed square beam of size 2–5 mm and a homogeneity degree exceeding 95%. The novel micro-lens array based on a cylindrical lens element can potentially be widely applied in practice because of the absence of the preparative limitations of size and focal length. By employing this beam homogenisation system, laser shock processing experiments were performed on 7050 titanium alloy. The laser shock processing parameters were optimised. When the laser repetition frequency was 1 Hz, pulse width was 15 ns, and laser energy was 20 J, a residual stress of $>$ 400 MPa was achieved on the titanium alloy. The experimental results demonstrate the ability of this beam-homogenisation system to perform laser shock processing.

1. Introduction

With the rapid development of laser technology, lasers have been widely used as a processing light source in many new fields, such as fabrication of micro-/nano-structures and patterns for various functional applications, long spot laser heating, and laser welding of copper materials[1–4]. Particularly in the field of aerospace, the use of lasers has attracted extensive attention. In recent years, more stringent requirements have been proposed for the reliability, fatigue strength, and service life of applied materials in the aerospace field[5–7]. Laser shock processing is a new surface treatment technology that has the potential to improve these features. It uses high-energy density and short-pulse laser irradiation on a metal material surface, thus subjecting the metal material to a high-strength pressure shock wave. The treated material surface forms a residual stress in the affected layer at a certain depth, which partially offsets the tensile stress and improves the fatigue strength, corrosion resistance, and wear resistance[8–10].

The traditional laser shock processing technology adopts Gaussian-distributed circular laser spots. However, in some cases, after the laser shock, the residual stress at the centre of the material is lower than at its edge, forming a "residual stress hole"[11]. Compared with a circular spot, a flat-top-distributed square spot has a more uniform residual stress field and cannot easily produce stress holes. Thus, the material characteristics are improved using this method. The beam homogenisation system is used in the free-running laser

* Corresponding author.
E-mail address: zhangjciomp@163.com (J. Zhang).

https://doi.org/10.1016/j.ijleo.2023.170525
Received 29 September 2022; Received in revised form 29 November 2022; Accepted 6 January 2023
Available online 7 January 2023
0030-4026/© 2023 Elsevier GmbH. All rights reserved.

Table 1
Typical parameters of high energy laser.

Parameters	Unit	Specifications
Output energy	J	0–30
Pulse width	ns	15
Repeat frequency	Hz	1–5
Beam size	mm	30
Spot divergence angle	mrad	0.5

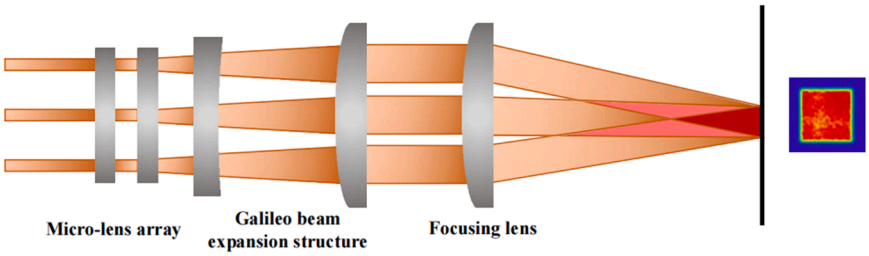

Fig. 1. Schematic of beam homogenisation based on a micro-lens array and Galileo beam expansion structure.

for beam shaping to obtain laser spots with a uniform energy distribution. The system typically includes a reflective integral mirror, waveguide integrator, segmentation superposition transformation system, and scanning vibrator[12–14]. In recent years, micro-lens arrays have been widely used in laser homogenisation owing to their rapid development. Wei et al. reported a facile design of highly integrated double-sided concave micro-lens arrays. These concave micro-lens arrays possess nearly 5000 close-packed micro-lenses on a double-sided glass substrate, which are created using a femtosecond laser wet-etch process. They exhibit excellent optical focusing performance and optical homogenisation[15]. Hsieh et al. presented micro-lens arrays with long focal lengths (in the millimetre range) based on a thermal reflow process. Micro-lenses of diameters from 50 μm to 240 μm were successfully fabricated, and the longest focal length was 2.1 mm using a micro-lens of diameter 240 μm. With this structure, the beam spot profile is symmetrical, indicating good quality of each lens in the micro-lens arrays[16]. However, these micro-lens arrays have certain disadvantages that limit their applications. On the one hand, the conventional preparation process of micro-lens arrays is relatively complex, with high processing difficulty and cost[17–19]. On the other hand, the focal length of traditional micro-lens arrays is limited, which restricts their application in optical shaping.

In this study, we propose an equivalent alternative plan with a simple structure, low lens processing difficulty, and low cost. Moreover, the cylindrical lens element adopted in this structure has no preparative limitations of size and focal length. Therefore, it is expected to be widely used in practice. A plano-concave cylindrical lens is used as a single-element device, and multiple plano-concave cylindrical lenses are spliced using optical glue. The combination of a plano-concave spliced cylindrical lens system and a Galileo beam expansion structure can convert circular spots into square spots. This method can obtain a good flat-top-distributed spot with a desired dimension. Thus, a beam shaping system for laser energies up to 30 J was designed, and the transformation of circular spots ϕ2–ϕ5 mm was realised. The circular–square spot was realised by combining it with a plano-concave cylindrical lens array. Square spots of 5 mm × 5 mm, 4 mm × 4 mm, 3 mm × 3 mm, and 2 mm × 2 mm were obtained with an energy uniformity greater than 95%. These results are conducive to improving the fatigue resistance and reliability of laser-enhanced materials.

2. Experimental principle and design

The technical parameters of the high-energy laser shock source are presented in Table 1. The pulse laser energy is 0–30 J, pulse width is 15 ns, repetition frequency is 1–5 Hz, initial spot diameter is 30 mm, and spot divergence angle is 0.5 mrad.

Fig. 1 shows a schematic of the experimental setup. Two plano-concave cylindrical micro-lens array structures are utilised in the system to reduce the processing cost and production difficulty and eliminate the preparative limitations of size and focal length that are inherent in traditional micro-lens processing methods. This process converts circular Gaussian spots into square flat-top spots. Multiple plano-cylindrical lenses are placed in each group and fixed using light glue. The two arrays of plano-concave cylindrical lenses are placed orthogonally to each other to divide the horizontal and vertical directions of the laser source and provide a uniform light effect in the system. To reduce energy loss when the laser beam passes the plano-concave spliced cylindrical lens system, the front and rear surfaces of the optical lenses are coated with anti-reflection films.

A beam expansion system is a key component of a laser shock processing system. The common beam expansion system includes the Kepler and Galileo expansion structures. A focus is formed between the two lenses when the Kepler beam-expansion structure is used. The focal system easily produces air breakdown near the focus under high-energy operation because the laser shock processing light source usually has high energy, small pulse width, and short pulse time. Therefore, it is unsuitable for use in the laser shock-processing system. The Galileo beam expansion structure consists of a positive focal objective and negative focal eyepiece. This structure, without focus, is suitable for use in this system because a confocal virtual focus is formed. The Gaussian-distributed laser beam during free

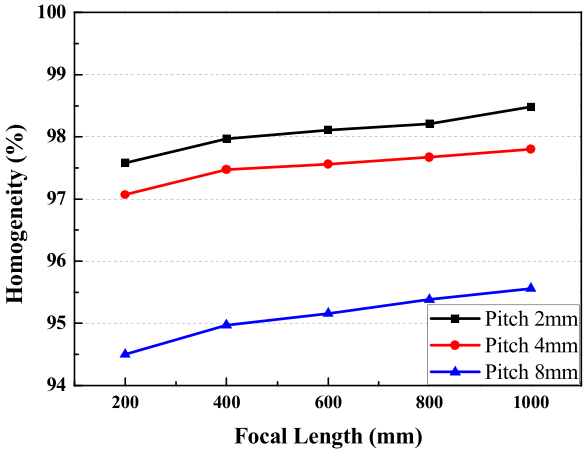

Fig. 2. Homogeneity of the focal beam with varying pitch and focal length of micro-lens array.

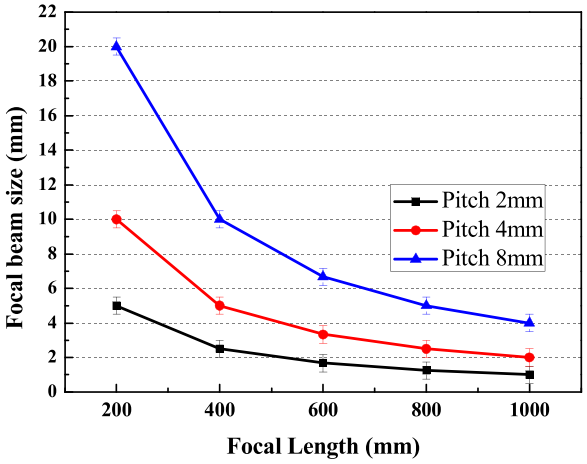

Fig. 3. Focal beam size with varying pitch and focal length of the micro-lens array.

running is first homogenised using a plano-concave spliced cylindrical lens group. The principle of the homogenised spot based on a plano-concave lens array is that the incident laser is divided into many small beams with a micro-lens array. These spots are amplified through the Galileo beam expansion system to reduce the divergence angle of the laser and are stacked together through the focusing lens[20,21]. Consequently, square spots with flat-top distributions are obtained.

The laser parameter product (*BPP*) is used to measure the beam quality[22], which is represented by Eq. (1). In the formula, ω_0 represents the waist radius of the laser beam, and θ represents the far-field divergence angle of the laser beam. That is, *BPP* is the product of the beam waist radius of the diode laser and the half-divergence angle of the far field[23]. In accordance with the principle of invariable beam quality, the product of the beam size and the spot divergence angle is constant. Therefore, the beam expansion can reduce the divergence angle of the laser and change the size of the focused beam.

$$BPP = \frac{\theta}{2} \cdot w_o \tag{1}$$

The uniform properties of the laser beam and the final focusing square spot size are associated with the period of the micro-lens array and focusing length of the micro-lens. The size of the square spot obtained after focusing is given by Eq. (2)[24]:

$$D = \left(\frac{p}{\beta}\right) \times \left(\frac{F}{f_m}\right) \tag{2}$$

where D is the focal spot size, p is the cycle of the micro-lens array, β is the spot magnification of the Galileo beam-expansion structure, F is the focal distance of the focusing lens after the Galileo beam-expansion system, and f_m is the focal distance of the micro-lens array. From the formula above, flat-top square spots of different sizes can be obtained by designing the period and focal length of the micro-lens, magnification of the Galileo beam expansion structure, and focusing lens after the beam magnification system.

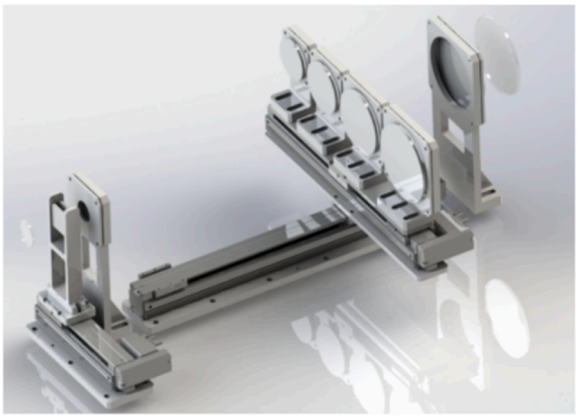

Fig. 4. Schematic of the laser shock beam shaping system.

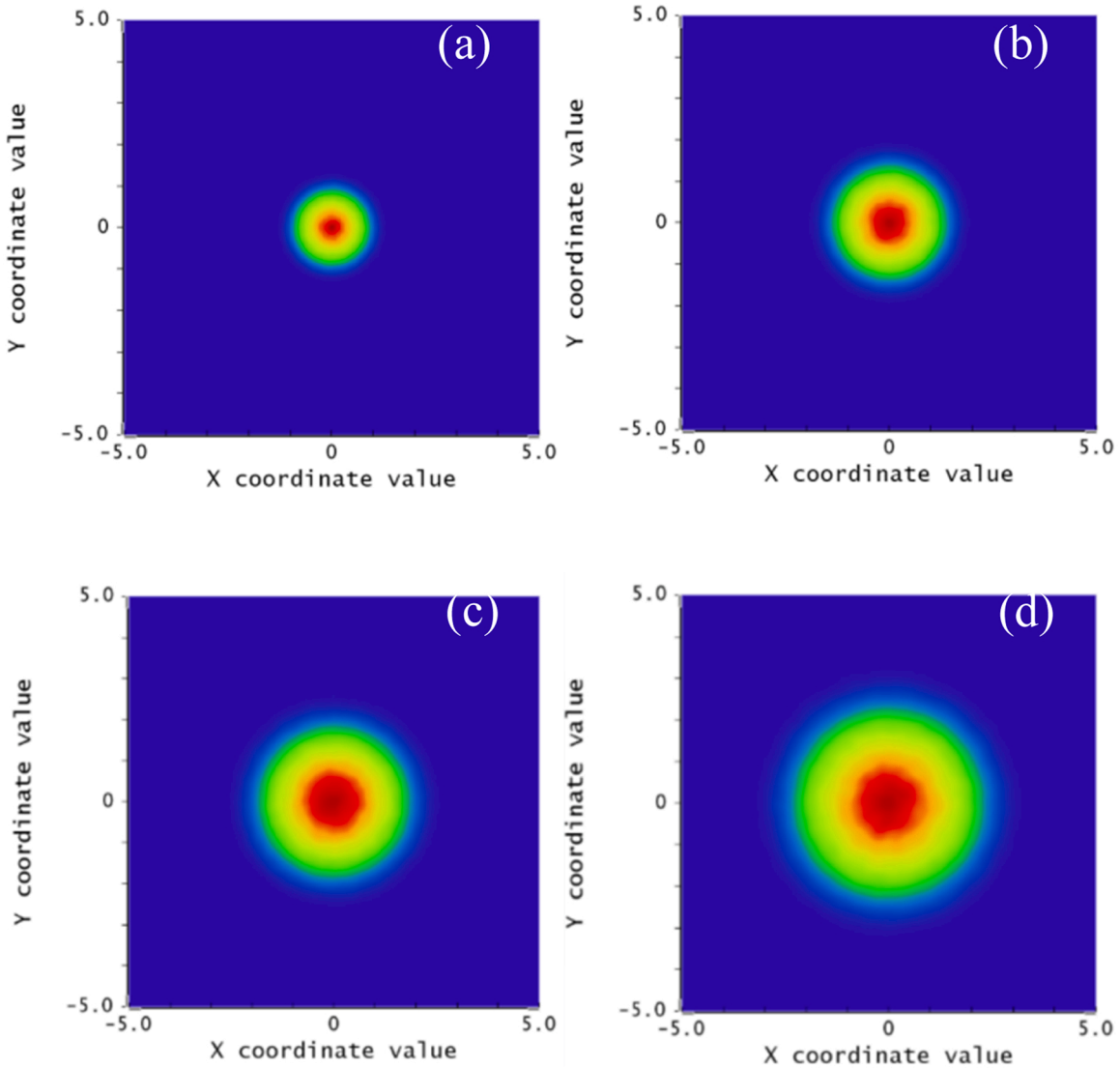

Fig. 5. Circular beam diagram of a Gaussian distribution with a varying focus lens position: (a) 2 mm (b) 3 mm (c) 4 mm, and (d) 5 mm.

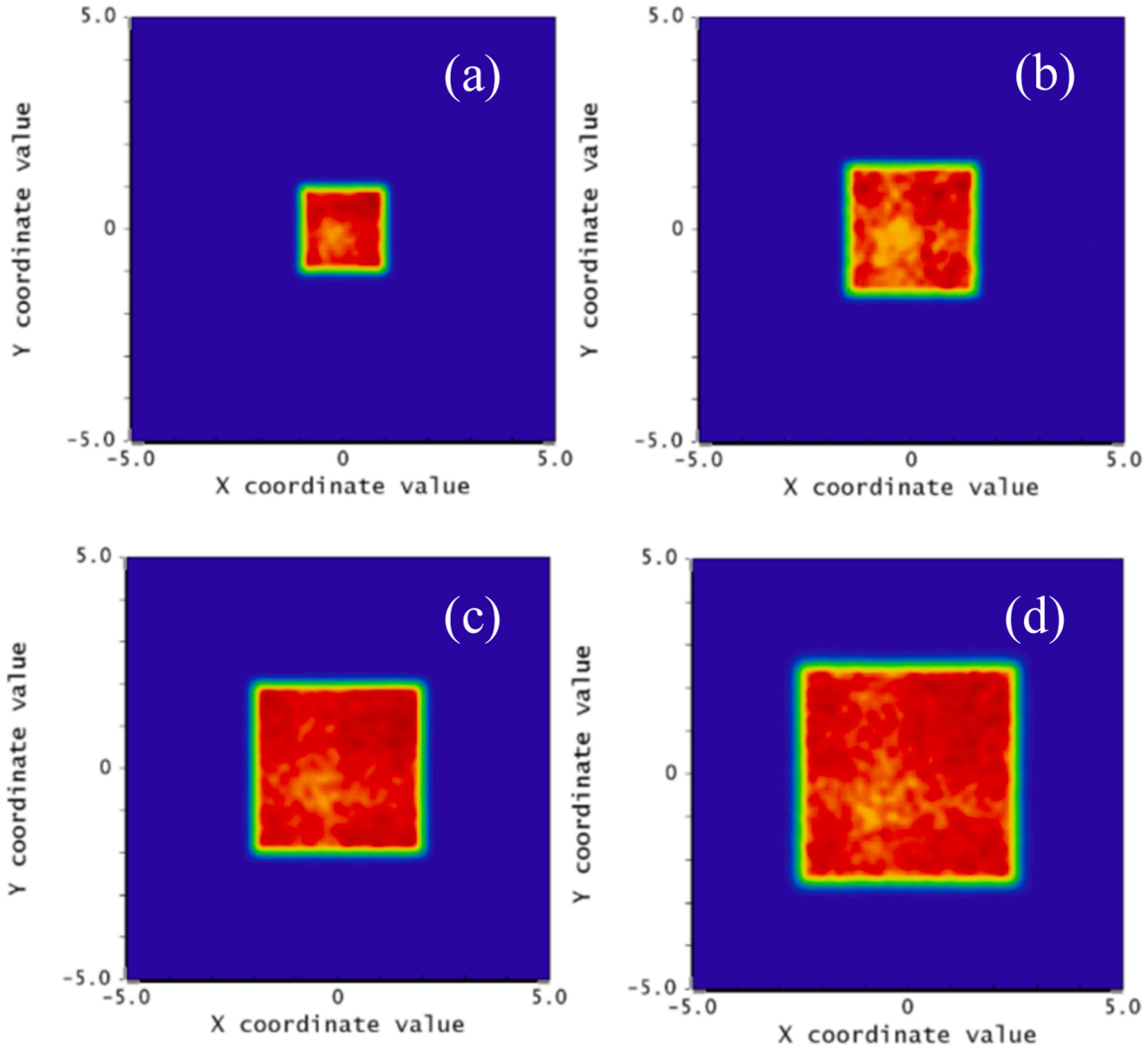

Fig. 6. Square beam diagram of a flat-top distribution with a varying Galileo beam expansion structure: (a) 2 mm (b) 3 mm (c) 4 mm, and (d) 5 mm.

The magnification ratio of the Galileo magnification system was set to two, and the focal length of the beam magnification system was 1 m. The micro-lens array spot sizes for different periods and focal lengths were simulated using ZEMAX software, and the uniform effect was analysed. The intensity distribution of the focused beam was evaluated in terms of its uniformity expressed as Eq. (3)[25]:

$$U = 1 - \frac{(I_{\max} - I_{\min})}{(I_{\max} + I_{\min})} \tag{3}$$

where, I_{max} and I_{min} represent the minimum and maximum intensity distributions, respectively. As shown in the simulation results in Fig. 2, all curves exhibit similar trends with changes in the focal length and period of the micro-lens array. The homogeneity of the focal spot increases significantly with decreasing period at the same focal length of the micro-lens array. In contrast, it increases linearly with increasing focal length at the same period of the micro-lens array. However, during the laser shock processing, the energy density decreases with an increase in the size of the focus spot under the same energy. Thus, a reasonable spot size must be designed in accordance with the requirements of the impact reinforcement material. As shown in Fig. 3, the effects of the micro-lens array focal length and period on the focal spot size are simulated. The spot size decreases with decreasing period at the same focal length of the micro-lens array. In contrast, it increases with increasing focal length at the same period of the micro-lens array.

The beam homogenisation system based on the micro-lens array structure is shown in Fig. 4. This system consists of an input lens, a micro-lens array group, a plano-concave lens, four collimating lenses, a focusing lens, an output lens, a straight-line slide, and a cross slide. All lenses are plated with an anti-reflection coating. In this study, square spots of 5 mm × 5 mm, 4 mm × 4 mm, 3 mm × 3 mm, and 2 mm × 2 mm were obtained by designing four groups of lens parameters for the Galileo beam expansion system. A circular laser spot ϕ2–ϕ5 mm could be obtained by changing the position of the objective in the Galileo beam expansion system under the condition

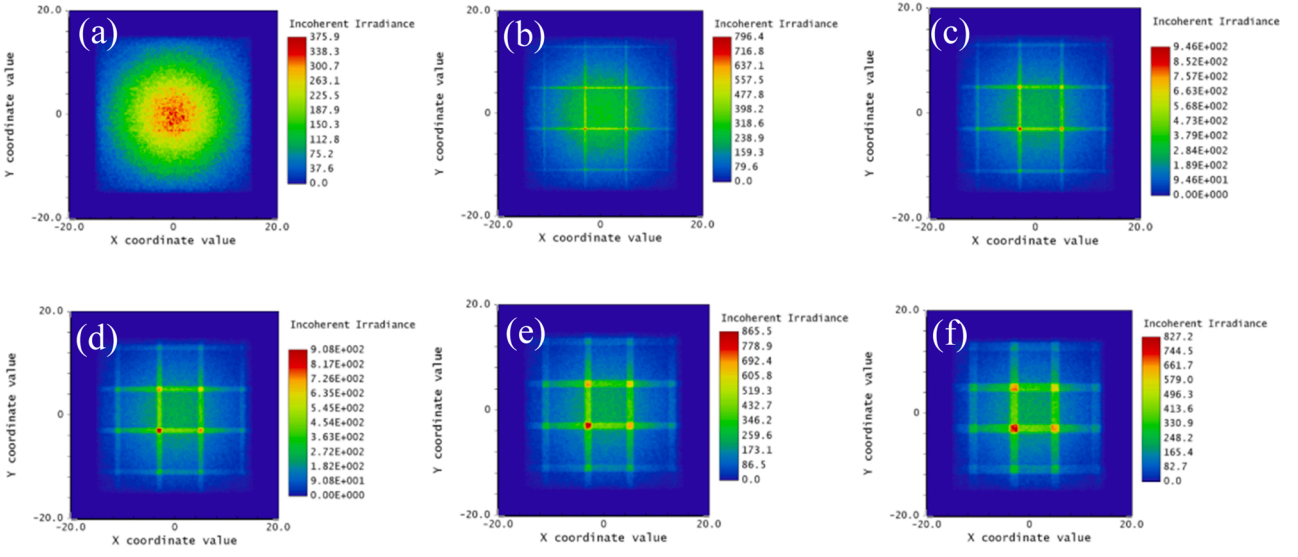

Fig. 7. Simulation results of the convergence effect with a varying position between the micro-lens arrays and the eyepiece of the Galileo beam expansion structure. (a) Incoherent irradiance: 375.9 (b) Incoherent irradiance: 796.4 (c) Incoherent irradiance: 946 (d) Incoherent irradiance: 908 (e) Incoherent irradiance: 865.5, and (f) Incoherent irradiance: 827.2.

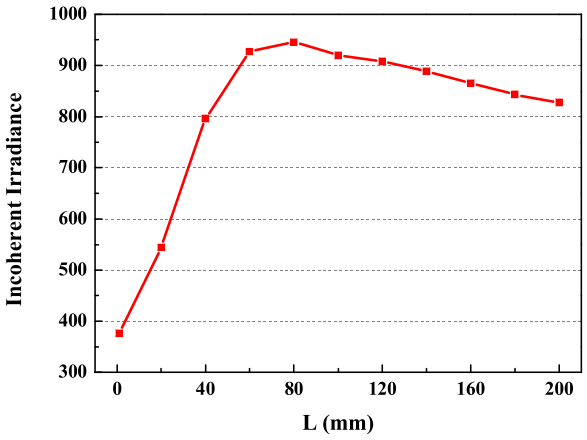

Fig. 8. Intensity distribution with a varying distance between the micro-lens arrays and the eyepiece of the Galileo beam expansion structure.

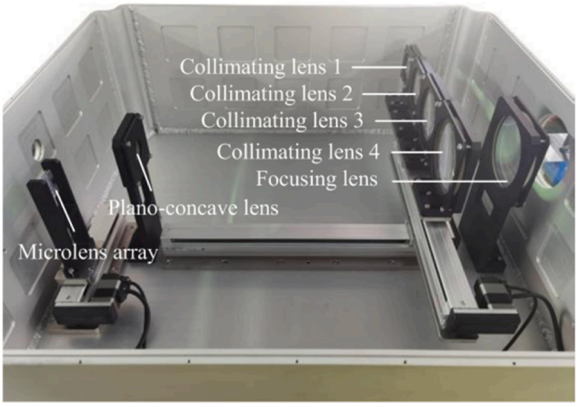

Fig. 9. Photograph of the beam-shaping system.

of either group of the aforementioned parameters.

3. Simulation and analysis

In accordance with the aforementioned analysis, because the initial beam size was 30 mm, the micro-lens array size was 40 mm × 40 mm, and the period was set to 8 mm. The focal length of the micro-lens array and the focusing lens at the end of the optical path were designed to be 1 m. As long as the divergence angle of the laser beam before the focusing lens was 5 mrad, the size of the square focusing spot was 5 mm × 5 mm. Similarly, square focusing spots of 4 mm × 4 mm, 3 mm × 3 mm, and 2 mm × 2 mm were realised by optimising the lens magnification in the Galileo beam expansion system. ZEMAX software was used to simulate a circular spot. To obtain a Gaussian-distributed beam, the micro-lens array group was removed, and the expanded spots were defocused by either collimating lens. The simulation results show that spot sizes of ϕ2–ϕ5 mm can be realised theoretically, as shown in Fig. 5.

To obtain a flat-top square spot, the micro-lens array group needs to be moved into the optical path. The intensity distribution of the square focus beam spot with 2, 3, 4, and 5 mm can be realised by switching collimating lens 1–4. The simulation results of the beam spot are shown in Fig. 6.

Considering the damage threshold for the lens coating, the entire optical path should be simulated and analysed because of the higher peak energy of the laser shock processing system. The strongest laser intensity distribution should occur before the plano-concave lens because this system is defocusing. Although the micro-lens array group uses a plano-concave structure to diverge the incident laser, the diverged laser converges in the near field. When the laser light source is converted into a square spot distribution, strong energy distributions are generated at the intersection of the square spots. The distance between the micro-lens array group and the first eyepiece in the Galileo beam expansion system significantly affects the energy distribution of the intersections. The simulation results are shown in Fig. 7.

As shown in Fig. 8, the peak energy intensity is low when approaching the distance between the micro-lens array group and the first eyepiece in the Galileo beam expansion system. With increasing distance, the peak energy intensity gradually increases and then decreases after 80 mm. The simulation results show that when the distance is 200 mm, the peak energy intensity remains higher than

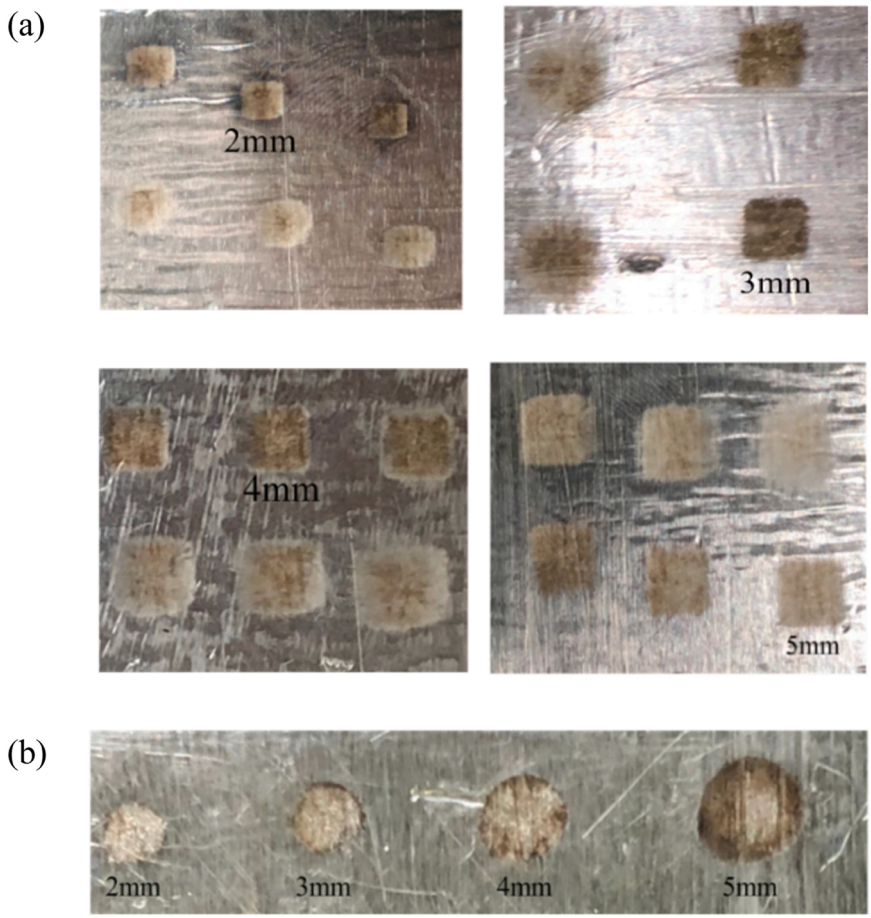

Fig. 10. (a) Photograph of a flat-top-distributed square beam from 2 mm to 5 mm. (b) Photograph of a Gaussian-distributed circular beam from ϕ2 mm to ϕ5 mm.

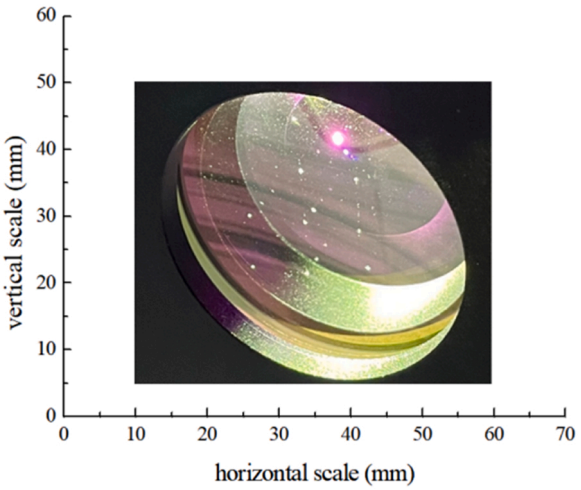

Fig. 11. Photograph of a laser-damaged lens by the convergence effect.

that at a distance of 20 mm. Considering the damage threshold of the plating, the distance between the micro-lens array group and the plano-concave lens should be less than 20 mm, and a smaller value is better for designing the optical and mechanical properties of the laser shock system.

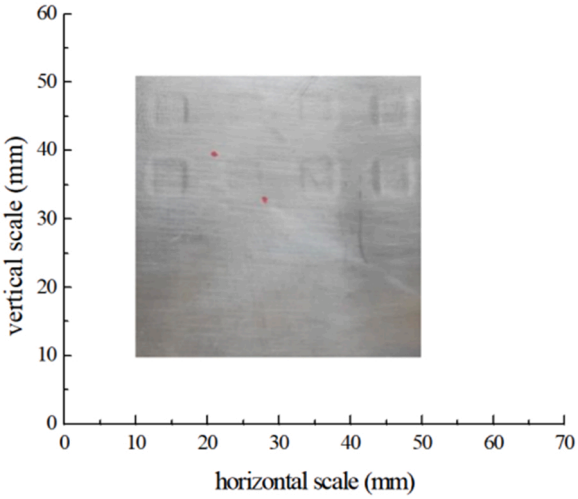

Fig. 12. Photograph of 7050 titanium alloy after laser shock processing.

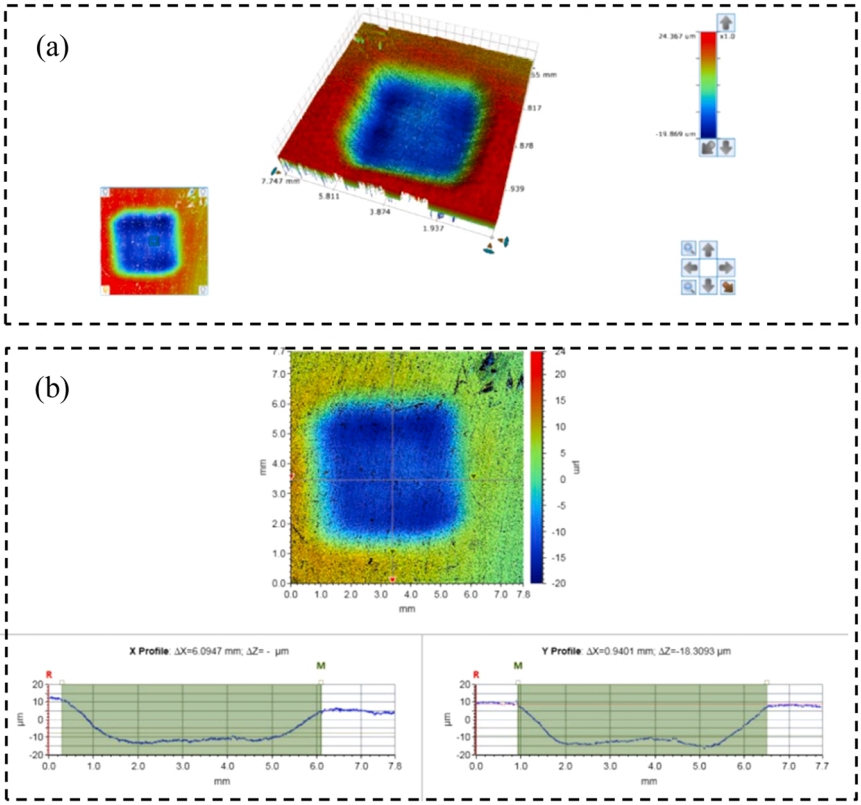

Fig. 13. (a) Test of the morphology of 7050 titanium alloy after laser shock processing. (b) Test of the cross section of 7050 titanium alloy after laser shock processing.

4. Results and discussion

The beam-shaping system designed in this study is illustrated in Fig. 9. The focal length of the micro-lens array and the focusing lens at the end of the optical path were designed to be 1 m. Collimating lens 1 with a focal length of 0.32 m was used in the square-spot regulation system to shape the laser beam into 5 mm. Collimating lenses 2–4 with focal lengths of 0.4, 0.53, and 0.8 m were used to shape the laser beam into 4, 3, and 2 mm, respectively. The straight slide, cross slide, and high-precision progress motor were equipped

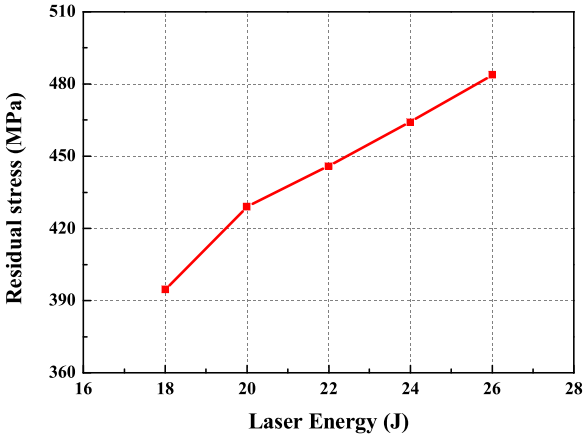

Fig. 14. Residual stress with a varying laser shock energy.

to achieve accurate adjustment of the square spots. The measured square spots are shown in Fig. 10(a). When the micro-lens array is moved out of the optical axis and one of the four collimators is arbitrarily selected for adjustment, a circular spot of ϕ2–ϕ5 mm in size can be obtained, as shown in Fig. 10(b).

A laser beam with a wavelength of 1064 nm, an energy of 30 J, and a pulse width of 15 ns was shaped. The micro-lens array group distance was set to 50 mm. When the laser energy was increased to 15 J, array-structure bad points occurred on the two plano-concave coating surfaces. By changing the lens angle and increasing the distance to 120 mm, bad points still occurred in the array structure, which coincided with the theoretical simulation results, as shown in Fig. 11. When the distance was reduced to 5 mm and the laser energy was set to 30 J, no undesirable points were observed. Therefore, the laser energy needs to be considered when using a micro-lens array structure for beam homogenisation and beam shaping. Although a single plano-concave cylindrical lens is a non-focus system, the overlap of the beam generated between them converges within a certain distance. The increase in the intensity originates from the overlapping areas of neighbouring sub-beams generated by the array structure. The overlap of the diverging sub-beams generates high intensities in the overlapping regions. When combined with the Galileo beam expansion structure for beam shaping, the position of an appropriate eyepiece should be selected. Otherwise, it is easy to cause coating damage to the lens and affect the final uniformity.

Laser shock experiments were performed on 7050 titanium alloy. The two sides of the substrate were polished before the laser shock and then wiped with alcohol. The samples after the shock reinforcement are shown in Fig. 12. The width of the laser impact spot was tested using a Contour GT white light interferometer produced by BRUKER to obtain 2D images of the sample surface under a 20 × lens. The obtained results are consistent with the simulation results. After the circle-square spot conversion, the laser beam with a Gaussian distribution is converted to that with a flat-top distribution, and the beam uniformity of the square spot is effectively improved after the beam shaping, as shown in Figs. 13(a) and 13(b).

The shock-spot residual stress of the experimental material was tested. The residual stress was tested using an LXRD high-power residual stress tester. Different residual stress values were measured at different laser energies, as shown in Fig. 14. The results demonstrate that the residual stress of the initial substrate was 33.4 MPa. When the laser repetition frequency was 1 Hz and the pulse width was 15 ns, the residual stress on the titanium alloy surface exceeded 400 MPa at an impact energy of > 20 J. A 10-fold improvement was achieved compared with the initial value. The fatigue resistance, strength, and wear resistance of the material were effectively improved by using this method.

5. Conclusion

In this study, a novel structure of a micro-lens array and beam expansion structure is proposed with the advantages of simple construction, convenient production, excellent homogenisation, and absence of the preparative limitations of size and focal length. Based on this beam homogenisation system, the conversion of a Gaussian-distributed circular beam to a flat-top-distributed square beam with a size of 2–5 mm and a homogeneity degree of $> 95\%$ was achieved. The laser energy intensity of the system was simulated considering the high energy of the laser source. The results demonstrate that the distance between the micro-lens arrays and the eyepiece in the Galileo expansion beam structure has a significant influence on the energy intensity. When the distance is less than 20 mm, the laser energy intensity in the optical path is lower. With increasing distance, the laser energy intensity increases significantly and decreases again after a certain distance. By exploring the parameters of laser shock processing of 7050 titanium alloy, a residual stress of more than 400 MPa was obtained at a laser repetition frequency of 1 Hz, pulse width of 15 ns, and laser energy of 20 J, which could effectively improve the fatigue resistance strength and wear resistance of the material. The experimental results demonstrate that the proposed beam-homogenisation system meets the requirements of industrial laser shock processing.

Funding

This work was supported by the Natural National Science Foundation of China (NSFC) (61991433 and 62121005), Project of CAS (XDB43030302 and YSBR-065), Equipment Pre Research (2006ZYGG0304 and 2020-JCJQ-ZD-245-11), Local Cooperation Projects of Chinese Academy of Sciences (2021SYHZ0012).

Declaration of Competing Interest

The authors declare that they have no known competing financial interests or personal relationships that could have appeared to influence the work reported in this paper.

Data Availability

No data was used for the research described in the article.

Acknowledgment

We thank our project partners for the assistance and fruitful discussions.

References

[1] Kai Yin, Zhipeng Wu, Junrui Wu, Zhuo Zhu, Fan Zhang, Ji-An Duan, Solar-driven thermal-wind synergistic effect on laser-textured superhydrophilic copper foam architectures for ultrahigh efficient vapor generation, Appl. Phys. Lett. 118 (21) (2021), 211905.
[2] Kai Yin, Lingxiao Wang, Qinwen Deng, Qiaoqiao Huang, Jie Jiang, Guoqiang Li, Jun He, Femtosecond laser thermal accumulation-triggered micro-/nanostructures with patternable and controllable wettability towards liquid manipulating, Nano-Micro Lett. 14 (2022) 97.
[3] Han Jinliang, Zhang Jun, Shan Xiaonan, Qin Li, Wang Lijun, High power heating light source based on semiconductor laser beam combintion technology, Acta Opt. Sin. 41 (2021), 221400.
[4] Yuta Ishige, Hiroshi Hashimoto, Naoki Hayamizu, Nobuyasu Matsumoto, Nishino, Fumika Blue, laser-assisted kW-class CW NIR fiber laser system for high-quality copper welding, Proc. SPIE 11668 (2021).
[5] A. Chattopadhyay, G. Muvvala, S. Sarkar, V. Racherla, A.K. Nath, Effect of laser shock peening on microstructural, mechanical and corrosion properties of laser beam welded commercially pure titanium, Opt. Laser Technol. 133 (2021), 106527.
[6] W. Jiajun, Z. Jibin, Q. Hongchao, L. Ying, S. Boyu, H. Taiyou, Z. Yinuo, The application status and development of laser shock processing, Opto-Electron. Eng. 45 (2018), 170690.
[7] B. Richter, S. Chen, J.D. Morrow, K. Sridharan, M. Eriten, F.E. Pfefferkorn, Pulsed laser remelting of A384 aluminum, part II: Modeling of surface homogenization and topographical effects, J. Manuf. Process. 32 (2018) 230–240.
[8] L. xuejun, Z. yinuo, W. jiajun, H. taiyou, Z. hongyao, L. changyun, W. lanjun, Research on principle and application of laser shock processing technology, Nonferrous Met. Process. 48 (2019) 10–15.
[9] H. Liu, C. Jiang, F. Liu, Y. Ma, X. Wang, Numerical and experimental investigations of laser shock hydraulic microforming for thin-walled foils, Thin-Walled Struct. 143 (2019), 106219.
[10] B. Wei, J. Xu, Y.F. Cheng, J. Wu, C. Sun, Z. Wang, Microstructural response and improving surface mechanical properties of pure copper subjected to laser shock peening, Appl. Surf. Sci. 564 (2021), 150336.
[11] G. Lu, L. Wang, H. Li, Z. Ji, Q. Wang, X. Pei, K. Sugioka, Methods for the suppression of “residual stress holes” in laser shock treatment, Materials Today, Communications 28 (2021), 102486.
[12] Y. Zhenyu, and S. Yan, Overview on Generators of Laser Surface Modification and Well-distributed Conversion System, Journal of Changchun Unicersity 25 (22015) 31–35.
[13] Z. Wang, G. Zhun, H. Yan, X. Zhu, C. Zhu, Analytical model of microlens array system homogenizer, Opt. Laser Technol. 75 (2015) 214–220.
[14] Z. Liu, H. Liu, Z. Lu, Q. Li, J. Li, A beam homogenizer for digital micromirror device lithography system based on random freeform microlenses, Opt. Commun. 443 (2019) 211–215.
[15] Yang Wei, Qing Yang, Hao Bian, Feng Chen, Minjing Li, Yanzhu Dai, Xun Hou, Fabrication of high integrated microlens arrays on a glass substrate for 3D micro-optical systems, Appl. Surf. Sci. 457 (2018) 1202–1207.
[16] H. Hsieh, V. Lin, J. Hsieh, G.J. Su, Design and fabrication of long focal length microlens arrays, Opt. Commun. 284 (2011) 5225–5230.
[17] Y. Liang, T. Zhu, M. Xi, H.N. Abbasi, J. Fu, R. Su, Z. Song, H. Wang, K. Wang, Fabrication of a diamond concave microlens array for laser beam homogenization, Opt. Laser Technol. 136 (2021), 106738.
[18] L. Jianjun, C. Chunyan, L. Weitong, Z. Pingping, Y. Gaoling, Z. Haizheng, Z. Yuejin, The developments of microlens array: from fabrications to photonic applications, Acta Opt. Sin. 41 (2021), 2100001.
[19] H. Yu, X. Ma, Y. Zou, L. Jin, Y. Xu, L. Xu, H. Zhang, Beam shaping design for fiber-coupled laser-diode system based on a building block trapezoid prism, Opt. Laser Technol. 109 (2019) 366–369.
[20] N. Yeh, Optical geometry approach for elliptical Fresnel lens design and chromatic aberration, Sol. Energy Mater. Sol. Cells 93 (2009) 1309–1317.
[21] F. Wang, L. Zhong, X. Tang, C. Xu, C. Wan, A homogeneous focusing system for diode lasers and its applications in metal surface modification, Opt. Laser Technol. 102 (2018) 197–206.
[22] B. Dai, Z. Zhou, Y. Long, M. Pan, Z. Song, D. Zhang, Multi-focused droplet lens array inspired by movable-type printing technology, Chin. Oprics Lett. 19 (10) (2021), 102201.
[23] Z. Wang, A. Segref, T. Koenning, R. Pandey, Fiber coupled diode laser beam parameter product calculation and rules for optimized design, Proc. SPIE 7918 (2011).
[24] Maik Zimmermann, Norbert Lindlein, Reinhard Voelkel, Kenneth J.Weible, Microlens laser beam homogenizer - from theory to application, Proc. SPIE 6663 (2007).
[25] Hongbo Zhu, Xihong Fu, Shengli Fan, Lei Liang, Xingchen Lin, Yongqiang Ning, The conversion from a Gaussian-like beam to a flat-top beam in the laser hardening processing using a fiber coupled diode laser source, Opt. Laser Technol. 125 (2020), 106028.